Biosensors and Bioelectronics 141 (2019) 111437

Contents lists available at ScienceDirect

Biosensors and Bioelectronics

journal homepage: www.elsevier.com/locate/bios

Quantitative detection and evaluation of thrombus formation based on electrical impedance spectroscopy

Jianping Li, Nen Wan*, Jianming Wen, Guangming Cheng, Lidong He, Li Cheng

Institute of Precision Machinery and Smart Structure, College of Engineering, Zhejiang Normal University, Jinhua, 321004, Zhejiang Province, China

ARTICLE INFO

Keywords:
Blood
Thrombus
Electrical impedance spectroscopy
Fibrin
Red blood cell
Biosensor

ABSTRACT

Thrombus formation is quantitatively measured and evaluated by the electrical impedance spectroscopy method in this study, which confirms the possibility for the application of a promising non-invasive thrombus detection method. The impedance parameter $Z^*(t)$ of blood from the electrical impedance spectroscopy is utilized to elaborate the impedance performance of blood during thrombus formation process. Experimental results indicate that the impedance $Z^*(t)$ of blood has regular variations under the formation of thrombus, which could be divided into three stages. Modified Hanai equation is proposed to quantitatively expound the three stages of impedance $Z^*(t)$ variation. The amount of fibrin and thrombus clot is founded to be accounted for the impedance variation of blood, which confirms the feasibility and theoretical basis of the non-invasive and on-line thrombus bio-detection technology for patients with serious cardiovascular disease.

1. Introduction

Cardiovascular diseases (CVDs) have become an extremely dangerous disease all over the world. According to the statistic study, CVDs are almost accounted for 32.3% of all the deaths in the United States (Go et al., 2013), and the total number of patients with CVDs in China has increased to 0.29 billion recent years (Chen et al., 2018). Among all the mortality caused by CVDs, thrombosis has been reported to play a significant role for the death of CVDs patients (Rhea et al., 2019; Teuteberg et al., 2017). How to measure the thrombus condition of patients in early stage has become the key therapy to save the life of patients with CVDs. Up to now, several methods have been developed by researchers to detect the thrombus condition of patients. According to the measurement principles, generally applied thrombus detection methods could be divided into thrombelastogram (TEG), computed tomography (CT), nuclear magnetic resonance imaging (MRI), optical coherence tomography (OCT), and ultrasound scanning. TEG is based on the mechanical force/torque measurement from the elasticity change of blood during blood coagulation, which makes it difficult to be utilized for compact on-line detection (Feller et al., 2014; Li et al., 2019). CT and MRI could obtain the micro structure of thrombus even inside patient's body (Heo et al., 2017; Maini et al., 2017). However, they always require quite expensive facilities, and the utilization of X-ray or other radiant rays may bring harm to human body. OCT exploits the light signal for tomography, but the light has the problem to penetrate the tissues and blood (Amabile et al., 2015; Imola et al., 2015). Ultrasound scanning has been widely utilized for thrombus detection, but it still has the difficult to distinguish the micro bubbles and thrombus clot (Fang et al., 2015; Hon et al., 2019).

Compared with the above methods for thrombus detection, electrical impedance spectroscopy (EIS) is appropriate for the non-invasive thrombus detection, due to the advantage that high frequency electrical signal has good penetration ability for tissues and blood (Wang et al., 2017). It is reported that EIS could distinguish the information of cells and even proteins easily (Oseev et al., 2017). Therefore, EIS is a promising method for on-line and non-invasive thrombus detection method for patients with CVDs. However, only a few researchers studied the possibility of EIS for thrombus detection (Asakura et al., 2015; Kailashiya et al., 2015). Additionally, the relationship between the impedance signal and thrombus formation process is still not explored clearly, which makes the theoretical basis of this promising on-line thrombus detection method missing. It means that why the impedance of blood changes during thrombus formation is still not clear, hence, the further application of the EIS measurement for thrombus detection is limited.

In this study, thrombus formation is quantitatively measured and evaluated based on the electrical impedance spectroscopy method. The experimental system with impedance analyzer is established to measure the impedance performance of blood during thrombus formation. The impedance signal $Z^*(t)$ under different input frequency f is recorded

* Corresponding author.
E-mail address: wannen@zjnu.cn (N. Wan).

https://doi.org/10.1016/j.bios.2019.111437
Received 20 April 2019; Received in revised form 6 June 2019; Accepted 12 June 2019
Available online 21 June 2019
0956-5663/

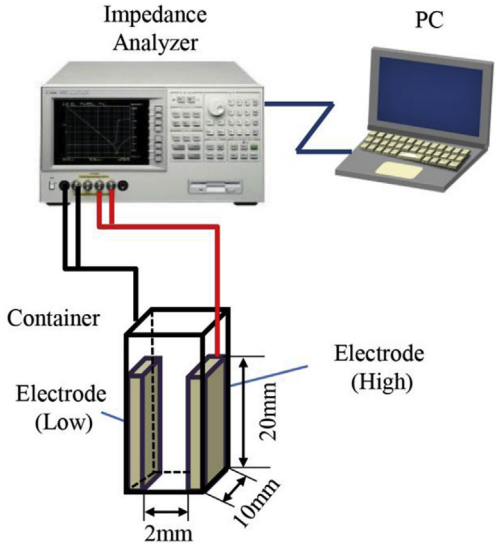

Fig. 1. Experimental setup of the electrical impedance measurement system for blood thrombus detection. (For interpretation of the references to colour in this figure legend, the reader is referred to the Web version of this article.)

and analyzed, and three variation stages of blood impedance $Z^*(t)$ are founded. In order to quantitative investigate the relationship between the impedance performance and thrombus formation process, the conventional Hanai equation is modified from the viewpoint of RBCs parameters (RBC orientation, RBC deformation, RBC electrical double layer (EDL) thickness). Finally, the modified Hanai equation is utilized to quantitatively analyze the variation of blood impedance during thrombus formation. This study shows new insights for the further development of a promising biosensing technology of on-line and non-invasive thrombus measurement for patients with CVDs based on the electrical impedance spectroscopy method.

2. Materials and methods

2.1. Experimental setup

Fig. 1 shows the experimental setup of the electrical impedance measurement system for blood thrombus detection. The experimental setup consists of a container with two electrodes, an impedance analyzer (IM7581, Hioki E.E. Corporation, Japan), and a personal computer (PC). During the experiments, blood is put inside the container which has a gap of 2 mm between the two electrodes. Additionally, the two electrodes of the container are connected with the impedance analyzer by two terminal probes. The input AC signal with high frequency is generated by the impedance analyzer, and the measured impedance signal of blood is also collected by the impedance analyzer. All the collected data are saved and processed by the PC. The size of the electrodes in the container is around 10 mm × 20 mm.

2.2. Blood samples

Due the ethical problem and the needed large amount, the porcine blood was utilized instead of human blood in the experiments. Porcine blood has been utilized to replace human blood in many early stage researches, since it is quite similar to human blood, especially for blood thrombus detection (Li et al., 2018a,b). The fresh blood sample was withdrawn from a porcine in the slaughterhouse in the early morning, and then mixed immediately with tri-sodium citrate solution (3.28%) to prevent the natural blood thrombus process. The volume ratio of blood and tri-sodium citrate solution is kept around 9:1. After that, the blood sample was transferred to the experimental lab in short time.

2.3. Experimental condition

Fresh porcine blood with 10% volume percent of 3.28% tri-sodium citrate solution was applied for the experiments. The hematocrit of the used porcine blood was around $H = 46.5\%$. During the experiments, 1 mL porcine blood (with tri-sodium citrate solution) was put inside the container. Then, 30 μL $CaCl_2$ solution with a weight fraction of 2% was added into the blood to generate thrombus. The input signal applied on the two electrodes of the container was an AC current with a value of $i = 0.1$ mA, and it swept from $f = 0.1$ MHz to $f = 300$ MHz (frequency scanning range of IM7581), which is used to obtain the suitable frequency range for blood impedance measurement.

3. Results

Fig. 2 illustrates the experimental results of the electrical impedance measurement during thrombus formation. As is mentioned in Part 2.3, porcine blood with a hematocrit of $H = 46.5\%$ was utilized for the measurement. $CaCl_2$ solution with a weight fraction of 2% was added into the porcine blood for the generation of blood thrombus. It is shown in Fig. 2 that the impedance $Z^*(t)$ of blood varies after the injection of $CaCl_2$ solution. Under the condition of different input frequencies, the variation of impedance $Z^*(t)$ is different. In the case that the input frequency is $f = 0.1$ MHz and $f = 0.5$ MHz, the impedance $Z^*(t)$ change of blood during thrombus formation is not notable. However, in the

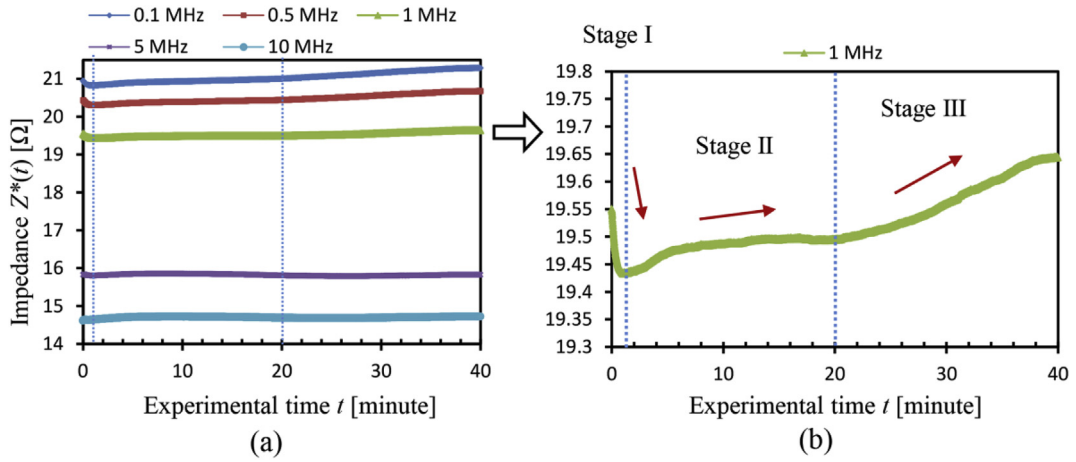

Fig. 2. Experimental results of the electrical impedance measurement for blood coagulation: (a) Impedance performance under different input frequencies; (b) Impedance performance under $f = 1$ MHz. (For interpretation of the references to colour in this figure legend, the reader is referred to the Web version of this article.)

case that the input frequency is $f = 1$ MHz, $f = 5$ MHz and $f = 10$ MHz, the impedance change is remarkable.

Fig. 2 (b) demonstrates the impedance $Z^*(t)$ performance during thrombus formation under the condition of input frequency $f = 1$ MHz. It is obvious that the change of impedance $Z^*(t)$ could be divided into three stages during the total measurement time of $t = 40$ min. At the first 2 min, after the injection of $CaCl_2$ solution, the impedance $Z^*(t)$ falls down quickly from $Z^*(t) = 19.55\,\Omega$ to $Z^*(t) = 19.43\,\Omega$. This is thought to be caused by the generation of fibrin. According to the theory of thrombus formation in previous studies, at the early stage, blood coagulation factors will react and the fibrinogen changes into fibrin which is confirmed by other researchers (Esther et al., 1999; Ahmad et al., 2017). The conductivity of fibrin is much larger than that of the fibrinogen, which brings the decreasing of blood impedance. The influence of fibrin is discussed in Section 4. After that, during the time $t = 2$ min to $t = 20$ min, the impedance $Z^*(t)$ increases slowly, which is caused by the generation of thrombus clot. Finally, during the time $t = 20$ min to $t = 40$ min, the impedance $Z^*(t)$ rises up quickly to the value of $Z^*(t) = 19.65\,\Omega$. This same variation trend of blood during thrombus formation also occurs under the input frequency of $f = 5$ MHz and $f = 10$ MHz. The variation of blood impedance $Z^*(t)$ during thrombus formation is thought to be induced by the generation and the amount of fibrin and thrombus clot, which will be quantitatively discussed in Part 4.

4. Discussion

In the experiments, the impedance $Z^*(t)$ of blood varies during thrombus formation, which is thought to be influenced by the fibrin and thrombus clot generation. According to precious studies, the thrombus formation process is quite complicated, many blood coagulation factors works together. Generally, in the case that thrombus generates, the fibrinogen in plasma develops into fibrin which has a fibrous structure. And then, blood cells are gathered together by the network of fibrin, which is the widely accepted thrombus formation process. Compared with other methods for thrombus detection, such as TEG method (Feller et al., 2014; Li et al., 2019), EIS method is more sensitive and it is able to detect the difference at the early stage, since the impedance changes immediately at the first stage. In order to quantitatively investigate the impedance change during blood coagulation, the modified Hanai equation is exploited to calculate the three stages shown in Fig. 2(b).

4.1. Modified Hanai equation

The conventional Hanai equation is generally utilized to calculate the colloid solution with high concentration. Here, the Hanai equation is modified to make it suitable for the calculation of blood. The modified Hanai equation is modified from the points of RBCs parameters (RBC orientation, RBC deformation, RBC EDL thickness) (Li et al., 2018a,b). However, the Hanai equation in that study is only available for the simplified blood model with the red blood cell and plasma, which means that it is only suitable for the model of a solution with one kind of cells. That research is used for the red blood cell aggregation investigation. It is not sufficient for the investigation of thrombus formation, which contains red blood cells, fibrin and plasma. In this study, the impedance $Z^*(t)$ of blood during thrombus formation could be calculated by the modified Hanai equation with the consideration of red blood cells, fibrin and plasma. Generally, more than 90% of the total blood cells in real blood are RBCs. In order to simplify the calculation, the whole blood is treated as the solution of RBCs and plasma. Before thrombus clot occures, fribrin generates quickly which could be simplified as in the long cylinder shape. Additionally, thrombus clot is treated as the coagulation of several RBCs. Here, the modified Hanai equation could be utilized for the calculation of the impedance change during thrombus formation process, which is shown as the following:

$$\left(\frac{\varepsilon^*_{blood}-\varepsilon^*_{RBC}}{\varepsilon^{F*}_{blood}-\varepsilon^*_{RBC}}\right)\left(\frac{\varepsilon^*_{blood}}{\varepsilon^{F*}_{blood}}\right)^{-C_1}\left(\frac{\varepsilon^*_{blood}+A'\varepsilon^*_{RBC}}{\varepsilon^{F*}_{blood}+A'\varepsilon^*_{RBC}}\right)^{-C_2}\left(\frac{\varepsilon^*_{blood}+B'\varepsilon^*_{RBC}}{\varepsilon^{F*}_{blood}+B'\varepsilon^*_{RBC}}\right)^{-C_3}=1-HCT \tag{1}$$

$$\left(\frac{\varepsilon^{F*}_{blood}-\varepsilon^*_{Fib}}{\varepsilon^*_{plasma}-\varepsilon^*_{Fib}}\right)\left(\frac{\varepsilon^{F*}_{blood}}{\varepsilon^*_{plasma}}\right)^{-C_{1F}}\left(\frac{\varepsilon^{F*}_{blood}+A_F{}'\varepsilon^*_{Fib}}{\varepsilon^*_{plasma}+A_F{}'\varepsilon^*_{Fib}}\right)^{-C_{2F}}\left(\frac{\varepsilon^{F*}_{blood}+B_F{}'\varepsilon^*_{Fib}}{\varepsilon^*_{plasma}+B_F{}'\varepsilon^*_{Fib}}\right)^{-C_{3F}}=1-H_{Fib} \tag{2}$$

where ε^*_{blood} is the permittivity of blood; ε^*_{RBC} is the permittivity of RBC; ε^{F*}_{blood} is the permittivity of the blood only with plasma and fibrin; ε^*_{plasma} is the permittivity of plasma; HCT is the hematocrit of blood; ε^*_{Fib} is the permittivity of fibrin; H_{Fib} is the volume percent of fibrin.

And ε^*_{RBC} could be obtained by the following equations:

$$\varepsilon^*_{RBC}=\varepsilon^*_m\frac{2(1-\nu)\varepsilon^*_m+(1+2\nu)\varepsilon^*_{cp}}{(2+\nu)\varepsilon^*_m+(1-\nu)\varepsilon^*_{cp}} \tag{3}$$

$$\nu=\frac{D_xD_yD_z}{(D_x+2d_x)(D_y+2d_y)(D_z+2d_z)} \tag{4}$$

where ε^*_{cp} is the permittivity of cytoplasm inside RBCs; ε^*_m is the permittivity of RBCs membrane; ν is the volume percent of cytoplasm inside RBCs; d_x, d_y, and d_z are the RBC EDL thickness in x, y and z axis, respectively.

Furthermore, ε^*_{plasma}, ε^*_{cp} and ε^*_m are obtained by the following:

$$\varepsilon^*_{plasma}=\varepsilon_{plasma}-j\frac{\sigma_{plasma}}{\omega\varepsilon_0} \tag{5}$$

$$\varepsilon^*_{cp}=\varepsilon_{cp}-j\frac{\sigma_{cp}}{\omega\varepsilon_0} \tag{6}$$

$$\varepsilon^*_m=\varepsilon_m-j\frac{\sigma_m}{\omega\varepsilon_0} \tag{7}$$

where ε_{plasma} and σ_{plasma} are the relative permittivity and relative conductivity of plasma, respectively; ε_m and σ_m are the relative permittivity and relative conductivity of RBCs membrane, respectively; ε_c and σ_c are the relative permittivity and relative conductivity of RBCs cytoplasm, respectively; ε_0 is vacuum permittivity (Bitbol and Quemada, 1985).

In this study, as mentioned above, blood is simplified as the solution of RBCs and plasma. RBCs are treated to be in the elliptical shape. Here, C_1, C_2 and C_3 are the deformation factors of RBCs which are obtained by the following:

$$C_1=\frac{L_xL_yL_z}{AB} \tag{8}$$

$$C_2=\frac{1+A'}{A(r)-B}\left(\frac{L_xL_yL_z}{A}-A^2+L_x(A-L_y)+L_y(A-L_z)+L_z(A-L_x)\right) \tag{9}$$

$$C_3=\frac{1+B'}{B(r)-A}\left(\frac{L_xL_yL_z}{B}-B^2+L_x(B-L_y)+L_y(B-L_z)+L_z(B-L_x)\right) \tag{10}$$

where L_x, L_y and L_z are the depolarization factors along the x, y and z axis of RBCs in terms of the elliptic integrals (Asami, 2002):

$$L_k=\frac{D_xD_yD_z}{2}\int_0^\infty\frac{ds}{(D_k^2+s)D_s},\ (k=x,y,z) \tag{11}$$

$$D_s=\sqrt{(D_x^2+s)(D_y^2+s)(D_z^2+s)} \tag{12}$$

where D_x, D_y, and D_z are the diameters of RBCs along x, y and z, respectively.

A' and B' are the orientation factors induced by the orientation of RBCs, as the following:

$$A' = \frac{b + \sqrt{b^2 - c}}{1 - b - \sqrt{b^2 - c}}, B' = \frac{b - \sqrt{b^2 - c}}{1 - b + \sqrt{b^2 - c}} \quad (13)$$

$$b = \frac{L_x(1 - \alpha_x) + L_y(1 - \alpha_y) + L_z(1 - \alpha_z)}{2} \quad (14)$$

$$c = \alpha_x L_y L_z + \alpha_y L_z L_x + \alpha_z L_x L_y \quad (15)$$

where α_x, α_y, and α_z are the RBCs in the direction of x, y and z axis, respectively. In this study, the blood is under the static condition, the orientation of RBCs is treated to be random ($\alpha_x = \alpha_y = \alpha_z = 1/3$). Additionally, the parameters C_{1F}, C_{2F}, C_{3F}, A_F' and B_F' for fibrin are obtained by same method according the radius and orientation of fibrin.

Based on the proposed modified Hanai equation, the impedance $Z^*(t)$ of blood could be obtained according to the following equation:

$$Z^*(t) = (j2\pi f A \varepsilon^*_{blood}/L)^{-1} \quad (16)$$

where A is the area of the electrode of the container; L is the distance between the two electrodes of container, which is shown in Fig. 1.

The parameters utilized in the calculation of blood impedance during thrombus formation based on the modified Hanai equation are shown in the Supplementary Material Table S1.

4.2. Calculation results

Fig. 3 illustrates the calculation results of the impedance performance during thrombus formation based on the modified Hanai equation. The calculation result in Fig. 3 shows great agreement with experimental result in Fig. 2(b). As shown in Fig. 3, the performance of blood relative impedance difference $\Delta Z_r^*(t)$ during thrombus formation process could be divided into three stages: in Stage I, the relative impedance difference $\Delta Z_r^*(t)$ of blood falls down quickly; in Stage II, it rises up slowly; in Stage III, the relative impedance difference $\Delta Z_r^*(t)$ of blood goes up quickly. And the relative impedance difference $\Delta Z_r^*(t)$ is obtained by the following:

$$\Delta Z_r^*(t) = \frac{Z_r^*(t) - Z_r^*(\min)}{Z_r^*(\min)} \times 100\% \quad (17)$$

where $Z_r^*(t)$ is the relative impedance under different time t; $Z_r^*(\min)$ is the minimum value of the impedance difference.

In order to quantitatively investigate the variation of blood impedance during thrombus formation, the modified Hanai equation is utilized according to the physiological process of thrombus formation. For normal blood, it could be treated as the solution of RBCs and plasma. At the beginning, the relative impedance $Z_r^*(t)$ of blood is set as $Z_r^*(t) = 1.00$. After the injection of $CaCl_2$ solution, $0 < t < 2$ min, fibrin generates quickly. Hence, during the calculation, fibrin with a cylinder shape is added in the blood together with the elliptical shaped RBCs. Subsequently, the relative impedance difference $\Delta Z_r^*(t)$ of blood from the calculation falls down from $\Delta Z_r^*(t) = 1.73\%$ to $\Delta Z_r^*(t) = 0$, which shows the same trend with the experimental results, as is shown in Fig. 3. The conductivity of fibrin is much larger than that of the fibrinogen, which brings the decreasing of blood impedance. Fibrin is thought to be responsible for the decreasing of $\Delta Z_r^*(t)$.

After that, about $t > 2$ min, thrombus clot is formed inside the blood. Therefore, besides the RBCs and fibrin, micro thrombus clot was added into the calculation which is treated as the coagulation of several RBCs. That is to say, thrombus clot brings the increasing of the relative impedance difference $\Delta Z_r^*(t)$ of blood, while fibrin make the relative impedance difference $\Delta Z_r^*(t)$ of blood decrease. Hence, during the Stage II, the relative impedance difference $\Delta Z_r^*(t)$ of blood only rises up slowly to around $\Delta Z_r^*(t) = 2.15\%$.

After $t > 20$ min, bigger thrombus clot is formed inside blood, while the amount of fibrin does not grow. The calculation result in Stage III illustrates a quick increase of blood relative impedance difference $\Delta Z_r^*(t)$ from $\Delta Z_r^*(t) = 2.15\%$ to $\Delta Z_r^*(t) = 4.55\%$, which is in agreement with the experimental result shown in Fig. 2(b).

From the calculation results in Fig. 3 and the experimental results in Fig. 2, it is confirmed that the generation of fibrin and thrombus clot brings the variation of blood impedance difference $\Delta Z_r^*(t)$. Namely, by measuring the variation of blood impedance difference $\Delta Z_r^*(t)$, the thrombus formation process could be detected by the electrical

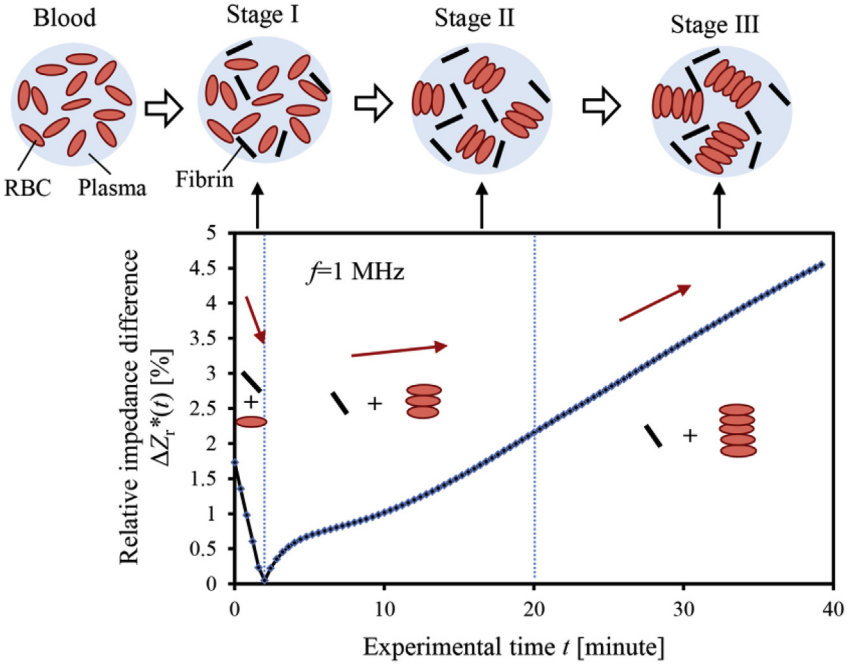

Fig. 3. Calculation results of the electrical impedance variation during thrombus formation based on the modified Hanai equation. (For interpretation of the references to colour in this figure legend, the reader is referred to the Web version of this article.)

impedance spectroscopy, which is a promising on-line and non-invasive thrombus detection method.

5. Conclusion

In this study, the impedance variation of blood during thrombus formation is measured by electrical impedance spectroscopy. The variation of blood impedance could be divided into three stages, and the conventional Hanai equation is modified to quantitatively calculate the impedance change of blood during thrombus formation. The generation of fibrin is verified to cause the decreasing of blood impedance in the case that $t < 2$ min after the $CaCl_2$ solution is injected. Meanwhile, micro thrombus clot has been confirmed to increase the impedance of blood during thrombus formation in the case that $t > 2$ min. This study shows the possibility and the theoretical evidence of the promising on-line and non-invasive detection method for thrombus formation based on electrical impedance spectroscopy.

CRediT authorship contribution statement

Jianping Li: Writing - original draft. **Nen Wan:** Conceptualization, Funding acquisition. **Jianming Wen:** Conceptualization, Funding acquisition. **Guangming Cheng:** Writing - review & editing. **Lidong He:** Data curation. **Li Cheng:** Data curation.

Acknowledgment

This work was supported by the Natural Science Foundation of Zhejiang Province: LY19E050010 and LY18E050012.

Appendix A. Supplementary data

Supplementary data to this article can be found online at https://doi.org/10.1016/j.bios.2019.111437.

References

Amabile, N., Hammas, S., Fradi, S., Souteyrand, G., Veugeois, A., Belle, L., Motreff, P., Caussin, C., 2015. Eur Heart J-Card Img 16 (4), 433–440.
Asakura, Y., Sapkota, A., Maruyama, O., Kosaka, R., Yamane, T., Takei, M., 2015. J. Artif. Organs 18 (4), 346–353.
Asami, K., 2002. J. Non-Cryst. Solids 305 (1), 268–277.
Ahmad, S.M., Roszymah, H., Kai, F.H., et al., 2017. AIP Adv. 7, 015202.
Bitbol, M., Quemada, D., 1985. Biorheology 22 (1), 31–42.
Chen, W., Gao, R., Liu, L., Zhu, M., Wang, W., Wang, Y., Wu, Z., Li, H., Gu, D., Yang, Y., Zheng, Z., Jiang, L., Hu, S., 2018. Chin. Circ. J. 33, 1–8.
Esther, A.R., Lyle, F.M., John, W.W., Laszlo, L., 1999. Biophys. J. 77, 2813–2826.
Fang, J., Wan, Y., Chen, C., Tsui, P., 2015. Biomed Res Int(403293).
Feller, T., Kellermayer, M.S.Z., Kiss, B., 2014. J. Struct. Biol. 186 (3), 462–471.
Go, A.S., Mozaffarian, D., Roger, V.L., Al, E., 2013. Circulation 127 (1), e6–e245.
Heo, J.H., Kim, K., Yoo, J., Kim, Y.D., Nam, H.S., Kim, E.Y., 2017. J. Stroke 19 (1), 40–49.
Hon, B., Botticello, A., Kirshblum, S., 2019. J. Spinalcord Med. 1–8.
Imola, F., Mallus, M.T., Ramazzotti, V., Manzoli, A., Di Vito, L., Occhipinti, M., Cremonesi, A., Kailashiya, J., Singh, N., Singh, S.K., Agrawal, V., Dash, D., 2015. Biosens. Bioelectron. 65, 274–280.
Kailashiya, J., Singh, N., Singh, S.K., Agrawal, V., Dash, D., 2015. Biosens. Bioelectron. 65, 274–280.
Li, J., Kikuchi, D., Sapkota, A., Takei, M., 2018a. Sensor. Actuator. B Chem. 268, 7–14.
Li, J., Sapkota, A., Kikuchi, D., Sakota, D., Maruyama, O., Takei, M., 2018b. Biosens. Bioelectron. 112, 79–85.
Li, Y., Chang, H., Ni, L., Xue, P., Li, C., Yuan, L., Cui, H., Yu, C., 2019. Exp Ther Med 17 (4), 3047–3052.
Maini, R., Gadiraju, T.V., Jabbar, A., Danrad, R., Sweeney, A., 2017. Int. J. Cardiovasc. Imaging 33 (11), 1795–1796.
Oseev, A., Schmidt, M.P., Hirsch, S., Brose, A., Schmidt, B., 2017. Sensor. Actuator. B Chem. 239, 1213–1220.
Rhea, I.B., Lyon, A.R., Fradley, M.G., 2019. Curr. Oncol. Rep. 21 (5), 45.
Teuteberg, J.J., Slaughter, M.S., et al., 2017. Biosens. Bioelectron. 90, 549–557.
Wang, X., Lin, G., Cui, G., Zhou, X., Liu, G.L., 2017. Biosens. Bioelectron. 90, 549–557.